THE INVERSE PROBLEM OF ELECTROENCEPHALOGRAPHY USING AN IMAGING TECHNIQUE FOR SIMULATING CORTICAL SURFACE DATA

C. Denson Hill, Ph. D.
Department of Mathematics, State University of New York at Stony Brook
Stony Brook, New York 11794 USA

R. Baker Kearfott, Ph. D., Robert D. Sidman, Ph. D.
Department of Mathematics, University of Southwestern Louisiana
USL Box 4-1010, Lafayette, Louisiana 70504 USA

Abstract

Evoked potential and EEG data consist of electrical potentials measured at a finite number of points (usually between 6 and 64) on the scalp. These data, obtained non-invasively, can be used to produce topographical potential plots to recognize neurological dysfunction.

The skull attenuates the potential fields generated by cortical and subcortical sources. It would therefore be desirable to obtain data directly from the cortical surface. However, this is only possible with invasive recording methods. In this work, we study a mathematical technique for computing approximate potential fields at the cortical surface, using only scalp-recorded potentials.

We report results of three preliminary experiments. In the first, we generate exact artificial scalp data from a known potential field and examine the error in the approximation. In the second, we generate scalp data, with and without simulated noise, from more than one separated source, and we examine the ability of our imaging technique to distinguish multiple sources not discernable from the raw scalp data. In the third, we apply the technique to data obtained by averaging actual measured potentials corresponding to left median nerve and right median nerve stimulation.

1. Description of the Technique

For now, we model the head by the unit ball in three dimensions; the x-axis points through the right ear, the y-axis points through the nasion, and the z-axis points through the vertex. The method depends on formulas by which we can explicitly compute the voltage at a point $A = (a_1, a_2, a_3)$ in this ball due to a current dipole with position vector $P = (p_1, p_2, p_3)$ and moment vector $M = (m_1, m_2, m_3)$ (cf. (2), (8), and (10)). We denote this voltage by $V(A, P, M)$.

The ideas behind our method are analogous to those in (3), (4), (6), and (7). We model the cortical surface by a spherical surface which, after correction for the skull's resistivity (see (1)) is at radius $r_I = .67$. We assume that the potential field is due to a distributed set of sources on a sphere of radius $r_T < r_I$. (The actual sources do not need to be on the sphere at r_I.)

We discretize the source field by assuming it is due to n current dipoles on the sphere with given positions $\{P_i\}_{i=1}^{n}$ and with moment vectors $\{M_i\}_{i=1}^{n}$ pointing radially outward but with unknown magnitudes $\{\mu_i\}_{i=1}^{n}$. Given the μ_i, we may compute the voltage at a point A_j on the scalp. Thus, if the electrodes are placed at $\{A_j\}_{j=1}^{m}$, and the measured voltages are $\{V_j\}_{j=1}^{m}$, the μ_i would need to satisfy each of the linear equations

$$\sum_{i=1}^{n} \mu_i V(A_j, P_i, \overline{M}_i) = V_j, \quad \text{for } 1 \le j \le m, \tag{1}$$

where $\overline{M}_i$ is the unit moment vector pointing radially outward from P_i.

In general, $m < n$ (since the points P_i are a discretization of a continuum), so (1) can be expected to be underdetermined. However, the system may in practice be numerically rank deficient. Also, solutions to (1) for which $\|(\mu_1, \mu_2, \ldots, \mu_n)\|_2$ is small will tend to correspond to potential fields with less artifactual bumps and wrinkles than solutions to (i) for which $\|(\mu_1, \mu_2, \ldots, \mu_n)\|_2$ is large. For these reasons, we use the singular value decomposition (SVD) (cf. e.g., (9) , pp. 317-326)) to compute the least squares solution of (1) of minimum norm.

An additional advantage of the SVD is that we can take account of noise in the data. Given an estimate ϵ_d of the relative errors in the data, we may replace the system in (1) by a (possibly) rank-deficient system such that errors of size ϵ_d will not unduly influence the solution.

Once the μ_i are computed, we use them, the formulas in (2), (8), and (10), and the principle of superposition to compute an approximation to the potential field on the cortical surface (i.e., on the sphere of radius r_I). We cannot take $r_T = r_I$ since the representation gives a more accurate approximation of the potential field a short distance away from the sphere at r_T.

In the experiments below, we define the points P_i in terms of the angles θ and ϕ in the standard spherical coordinate system. Unless otherwise indicated, we use 10 points on the θ arcs and 16 points on the ϕ arcs (so $n = 160$). The P_i thus have spherical coordinates

$$(r_T, \theta_k, \phi_\ell), \quad \theta_k = (k-1)(2\pi/10), \quad 1 \le k \le 10,$$
$$\phi_\ell = \ell(\pi/2)/16, \quad 1 \le \ell \le 16.$$

We compute potential values on the cortical surface over a similar grid.

We took as scalp recording sites 28 lead positions --either standard International 10-20 electrode positions or derivable from them.

We ran VS Fortran programs on the IBM 3090 at the University of Southwestern Louisiana; we used the LINPACK routine DSVDC (in (5)) for the SVD. In all experiments with $n = 160$, it took less than 4 seconds of CPU time to generate the approximate potential field.

We generated surface and contour graphs using SAS/GRAPH.

2. Experiments to Determine Attainable Accuracy

In these experiments, we generated data at the 28 lead coordinates listed above due to a current dipole at $(0, 0, r_D)$ with moment vector $(0, 0, 1)$. We then used the procedure outlined above (assuming noise ratio $\epsilon_d = 0$) to get an approximate potential field on the cortical surface, which we compared to the actual potential field due to the dipole. We defined the relative error to be the absolute value of the maximum difference divided by the absolute value of the maximum of the actual potential over the grid we placed on the cortical surface. For $r_D = .2$, $r_D = .4$, and $r_D = .6$, we studied the relative error as we varied the radius r_T of the test surface.

In Table 1, with $r_D = .2$, the potential field on the cortical surface is relatively smooth and flat (see Figure 1). In Table 2, $r_D = .4$; we see a surface plot of the actual potential distribution in Figure 2.

Table 1

no.	r_T	rel. err.
1.	.2	9.1×10^{-4}
2.	.25	2.3×10^{-4}
3.	.3	4.6×10^{-4}
4.	.4	106.2×10^{-4}

Table 2

no.	r_T	rel. err.
1.	.44	28.8×10^{-3}
2.	.45	25.1×10^{-3}
3.	.475	14.5×10^{-3}
4.	.5	6.7×10^{-3}
5.	.6	42.1×10^{-3}

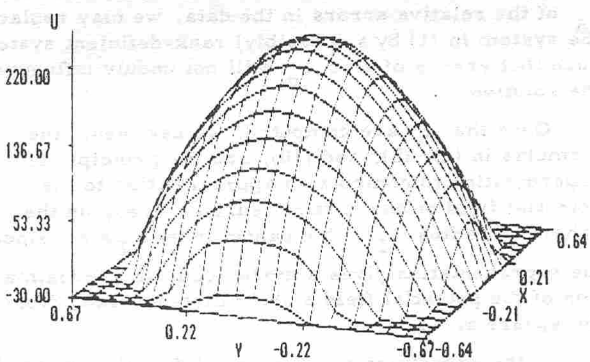

Figure 1

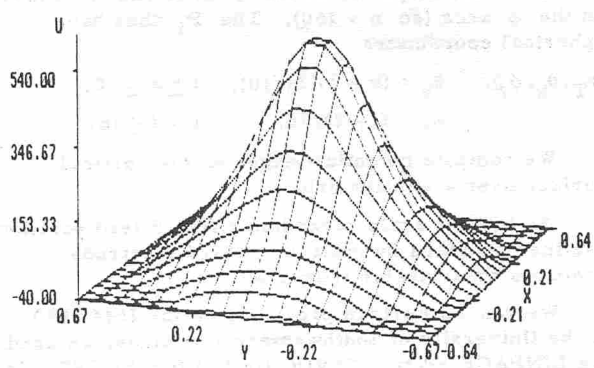

Figure 2

A surface plot of the approximate potential distribution with $r_D = .4$ and $r_T = .5$, is indistinguishable from the plot of the exact potentials in Figure 2. In Table 3, $r_D = .6$. This represents a potential field on the cortical surface which is a sharp spike (see Figure 3).

Table 3

no.	r_T	rel. err.
1.	.5	4.2×10^{-1}
2.	.55	3.8×10^{-1}
3.	.6	3.0×10^{-1}
4.	.61	2.6×10^{-1}
5.	.62	2.2×10^{-1}
6.	.63	1.9×10^{-1}
7.	.64	1.2×10^{-1}
8.	.65	2.3×10^{-1}

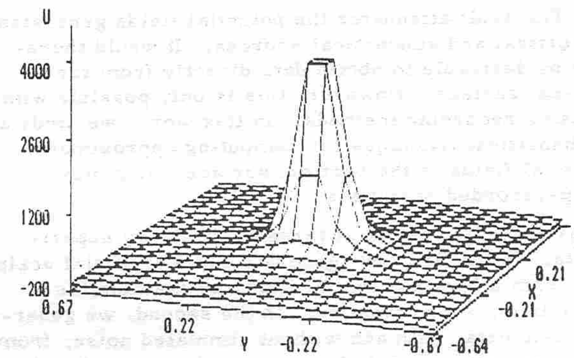

Figure 3

It seems from Tables 1, 2, and 3 that the optimal r_T is nearer the cortical surface when the potential field is less flat. Furthermore, in such cases, the minimum relative error is larger. We note that putting the test surface deeper smooths the potential distribution on the cortical surface.

When the test surface is near the cortical surface, the granularity of the discretization on the test surface may affect the results. Initial experiments along these lines are inconclusive. We note that (1) and the formula for computing voltages on the cortical surface, given the μ_i are really quadrature formulas. Thus, for many data sets, we could improve the results by using Gaussian points and weights on the ϕ arcs.

3. Experiments to Determine Ability to Separate Sources

We ran various experiments with multiple sources and simulated noisy data. We exhibit results here for data generated from two dipoles, one at $(0, -.2\sqrt{2}, .2\sqrt{2})$ and one at $(0, .2\sqrt{2}, .2\sqrt{2})$, and each with moment vector $(0, 0, .1)$. To the data on the surface of the skull, we added uniform pseudorandom noise with maximum deviation equal to 10% of the maximum true voltage. Figure 4 is a contour plot of the actual data on the surface of the skull, while Figure 5 is a contour plot of the approximate potential field on the cortical surface. We used $r_T = .5$ and $\epsilon_d = .1$; this resulted in an effective rank of 13 (where the full rank is 28). Increased definition of features is apparent.

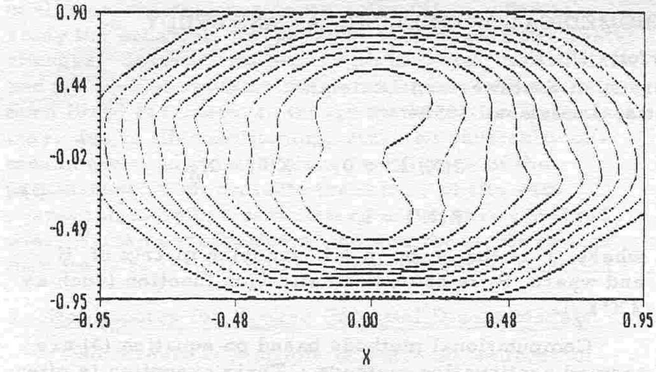

Figure 4

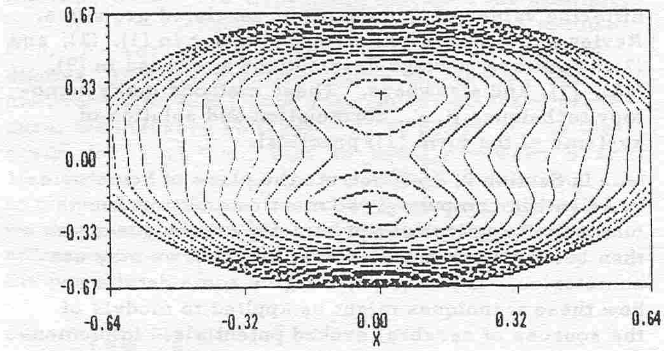

Figure 5

We note that the stretching in the x-direction is an artifact of the contouring routine, which we chose by convenience. Also, that routine fits the point data with cubic splines; that process may occasionally introduce artifactual bumps in the contours. We finally note that the image definition in a contour plot may depend on the number of contours plotted. We attempted to scale the plots so that, for both the actual data and for the approximate field on the cortical surface, we exhibit about 15 equally spaced contours.

4. An Experiment on Actual Data

In this experiment, we began with two evoked potential datasets with data at 36 scalp leads; the two sets represented left median nerve and right median nerve stimulation. (We obtained this data in 1980 from the West Haven, Connecticut, Veterans Administration Medical Center.) We averaged the voltages at each of the two lead sets to obtain simulated simultaneous stimulation. Since there appeared to be a significant amount of noise in this data, it was necessary to estimate the noise ratio. We took $r_T = .5$ and $\epsilon_d = .1$; this gave a numerical rank of 12. A contour plot of the approximate potential field on the cortical surface appears in Figure 6, while a contour plot based on the data at the surface of the skull appears in Figure 7. These plots hint at the possibilities of the method to both define and smooth the image of the potential field.

Acknowledgment

This work is partially supported by the Oregon Comprehensive Epilepsy Program, Good Samaritan Hospital, Portland, Oregon.

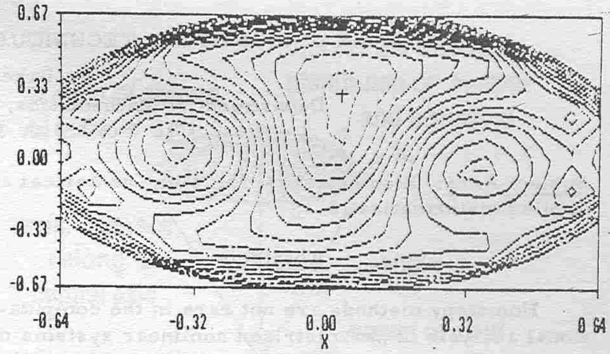

Figure 6

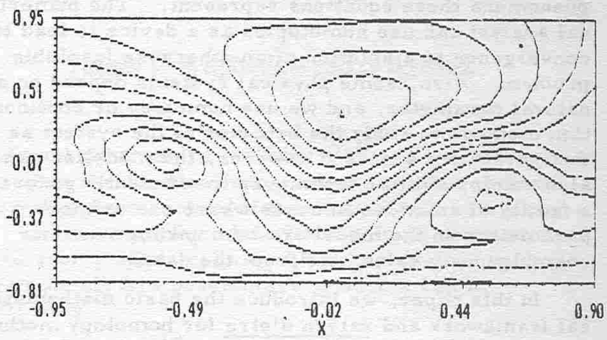

Figure 7

References

1. J.P. Ary, S.A. Klein, and D.H. Fender, "Location of sources of evoked scalp potentials: corrections for skull and scalp thicknesses," IEEE Trans. Biomed. Eng. 28, pp. 447-452, 1981.
2. D.A. Brody, F.H. Terry, and R.E. Ideker, "Eccentric dipole is a spherical medium: generalized expression for surface potentials," IEEE Trans. Biomed. Eng., pp. 141-143, 1973.
3. J.R. Cannon, "Some numerical results for the solution of the heat equation backward in time," in Numerical Solutions of Nonlinear Differential Equations, ed. D. Greenspan, John Wiley & Sons, 1967, pp. 21-54.
4. J.R. Cannon and J. Douglas, "The approximation of harmonic and parabolic functions on half-spaces from interior data" (CIME 2° Ciclo, 1967), Edizioni Cremonese, 1967, pp. 193-230.
5. J.J. Dongarra, C.B. Moler, J.R. Bunch, and G.W. Stewart, LINPACK Users' Guide, SIAM, Philadelphia, 1979.
6. J. Douglas, "Mathematical programming and integral equations," Symposium Provisional International Computation Center, Birkhäuser Verlag, Basel, 1960.
7. J. Douglas, "A numerical method for analytic continuation," in Boundary Value Problems in Differential Equations, University of Wisconsin Press, pp. 179-189, 1960.
8. E. Frank, "Electric potential produced by two point current sources in a homogeneous conducting sphere, Journal of Applied Physics, 23, 11, pp. 1225-1229, 1952.
9. G.W. Stewart, Introduction to Matrix Computations. Academic Press, 1973, New York.
10. F.N. Wilson and R.H. Bayley, "The electric field of an eccentric dipole in a homogeneous spherical conducting medium, "Circulation 1, 84-92, 1950.